Non-Gaussian deflections in optimal CMB lensing reconstruction

Omar Darwish
University of Geneva

Swiss National Science Foundation

Work with

Sebastian Belkner, Louis Legrand, Julien Carron, Giulio Fabbian

One of the goals of CMB-S4

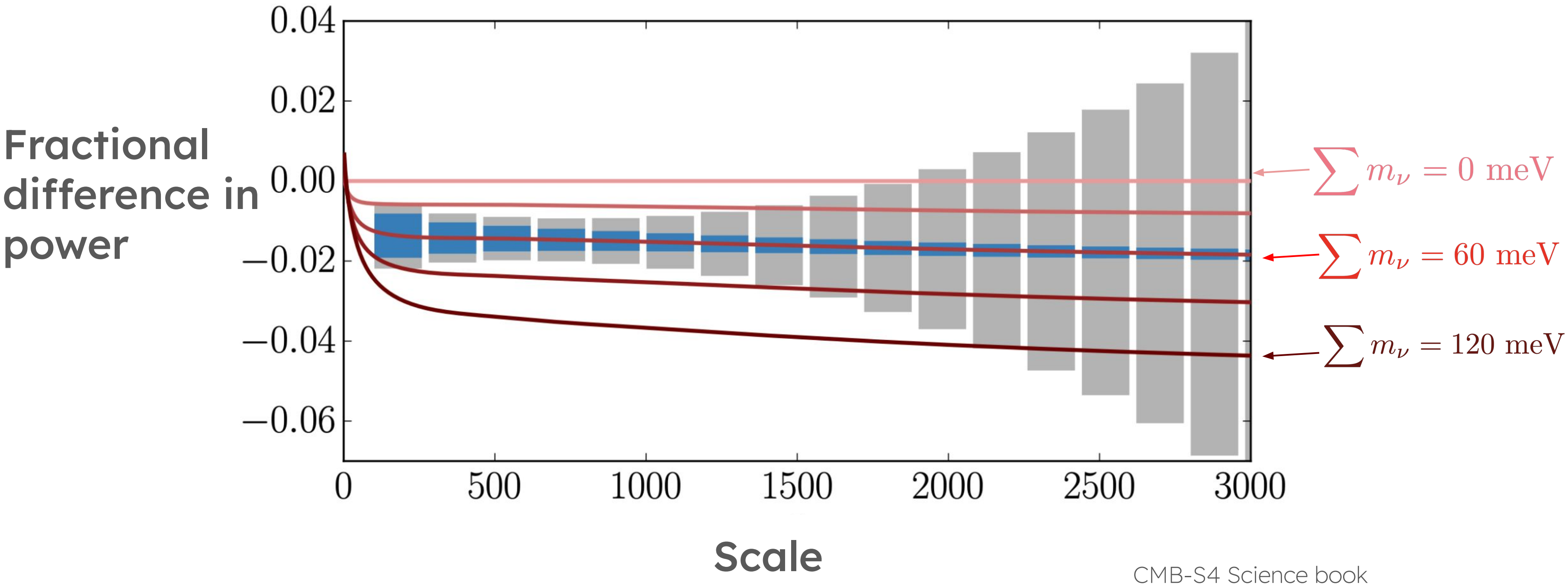

CMB-S4 Science book

Use QE CMB lensing estimator

$$\ln \mathcal{L} \supset -\frac{1}{2} X^{\mathrm{dat}} \cdot \mathrm{Cov}_{\kappa}^{-1} \mathrm{X}^{\mathrm{dat}} - \frac{1}{2} \mathrm{det} \mathrm{Cov}_{\kappa}$$

Maximize

$$\hat{\kappa}_{\mathrm{QE}} \sim \bar{X}^{\mathrm{dat}} \, \bar{X}^{\mathrm{dat,WF}} \times \mathrm{Norm}$$

First step of a Newton iteration
starting from no lensing

The QE CMB lensing estimator

$$\hat{\kappa}_{\rm QE} \sim \bar{X}^{\rm dat}\,\bar{X}^{\rm dat,WF} \times \mathrm{Norm}$$

by construction misses info in $\phi^2, \;\ldots.$

but also $XXX, \; XXXX, \; \ldots$

MAP CMB lensing estimator

$$\ln p \supset -\frac{1}{2} X^{\mathrm{dat}} \cdot \mathrm{Cov}_{\kappa}^{-1} \mathrm{X}^{\mathrm{dat}} - \frac{1}{2} \mathrm{det}\mathrm{Cov}_{\kappa} + \ln \mathrm{p}_{\mathrm{prior}}$$

$$\Downarrow \text{ Maximize}$$

$$\hat{\kappa}_{\mathrm{MAP}} \sim \bar{X}^{\mathrm{dat}}_{\hat{\kappa}_{\mathrm{MAP}}} \bar{X}^{\mathrm{dat}}_{\hat{\kappa}_{\mathrm{MAP}}} \times \mathrm{Norm}$$

Carron, Lewis (2017)

MAP CMB lensing estimator

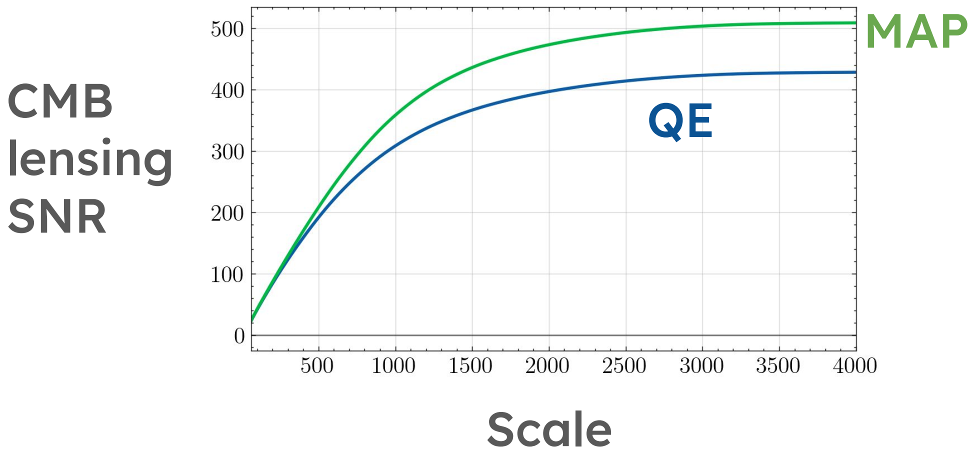

$$\hat{\kappa}_{\mathrm{MAP}} \sim \bar{X}^{\mathrm{dat}}_{\hat{\kappa}_{\mathrm{MAP}}} \bar{X}^{\mathrm{dat}}_{\hat{\kappa}_{\mathrm{MAP}}} \times \mathrm{Norm}$$

Carron, Lewis (2017)

One of the goals of CMB-S4

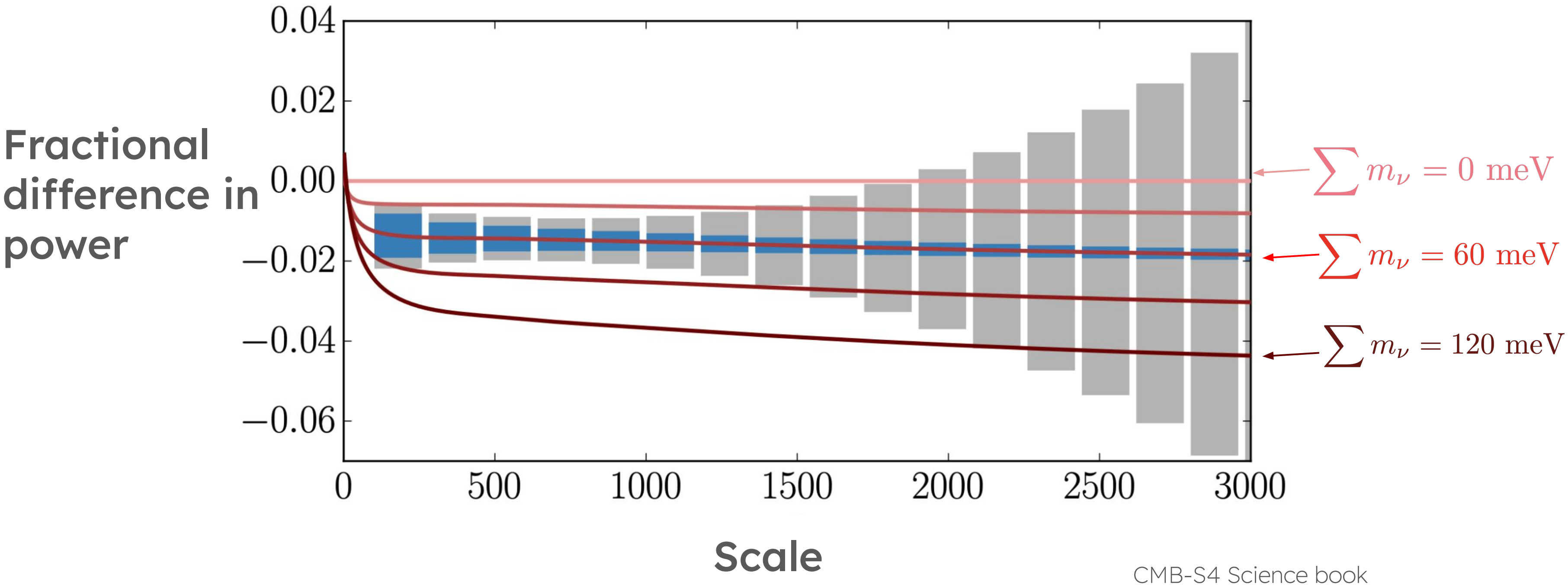

CMB-S4 Science book

Beyond Gaussian mass map

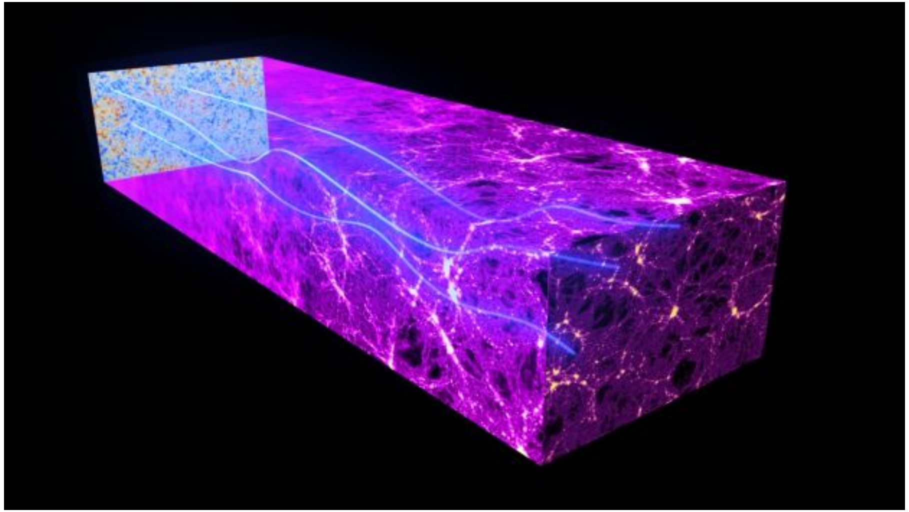

ESA and the Planck Collaboration

Projected non-Gaussian large scale structure

Beyond Gaussian mass map

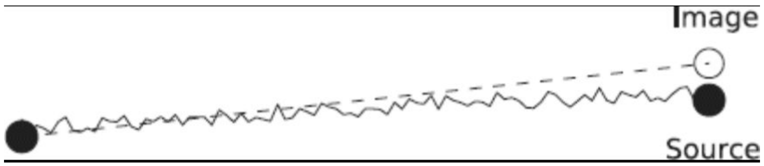

Credit S. Dodelson

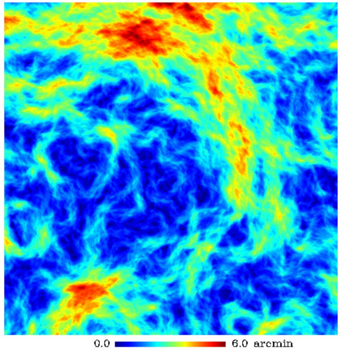

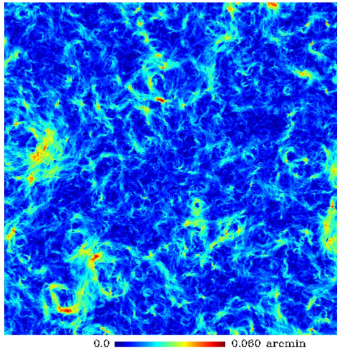

Amplitude of Post Born corrections

Credit G. Fabbian

Pratten, Lewis (2016)

Beyond Gaussian mass map

Non-Gaussian lensing from simulations

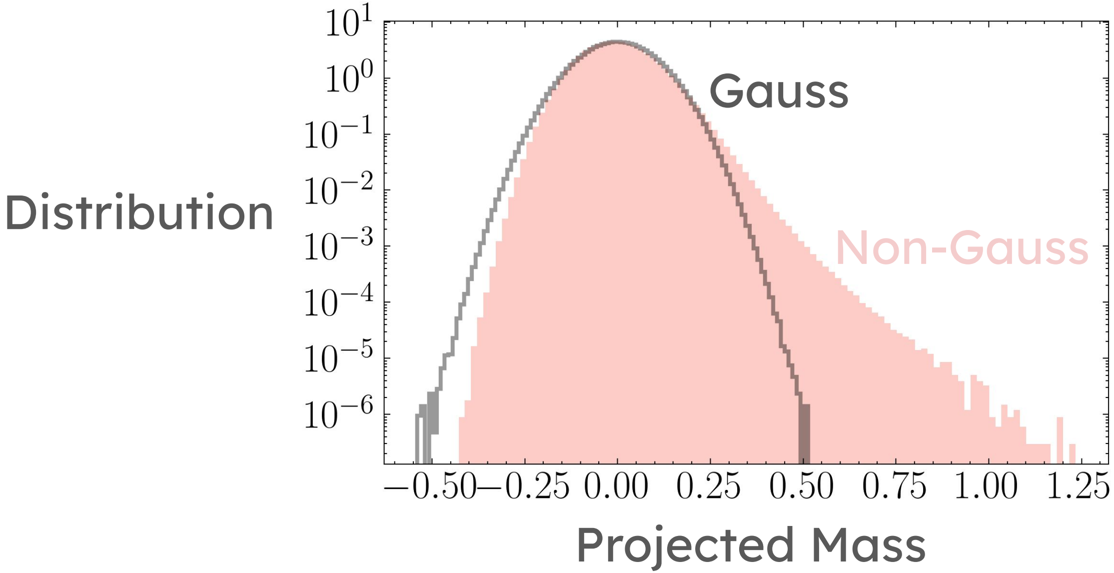

Impact of non-Gaussian deflections

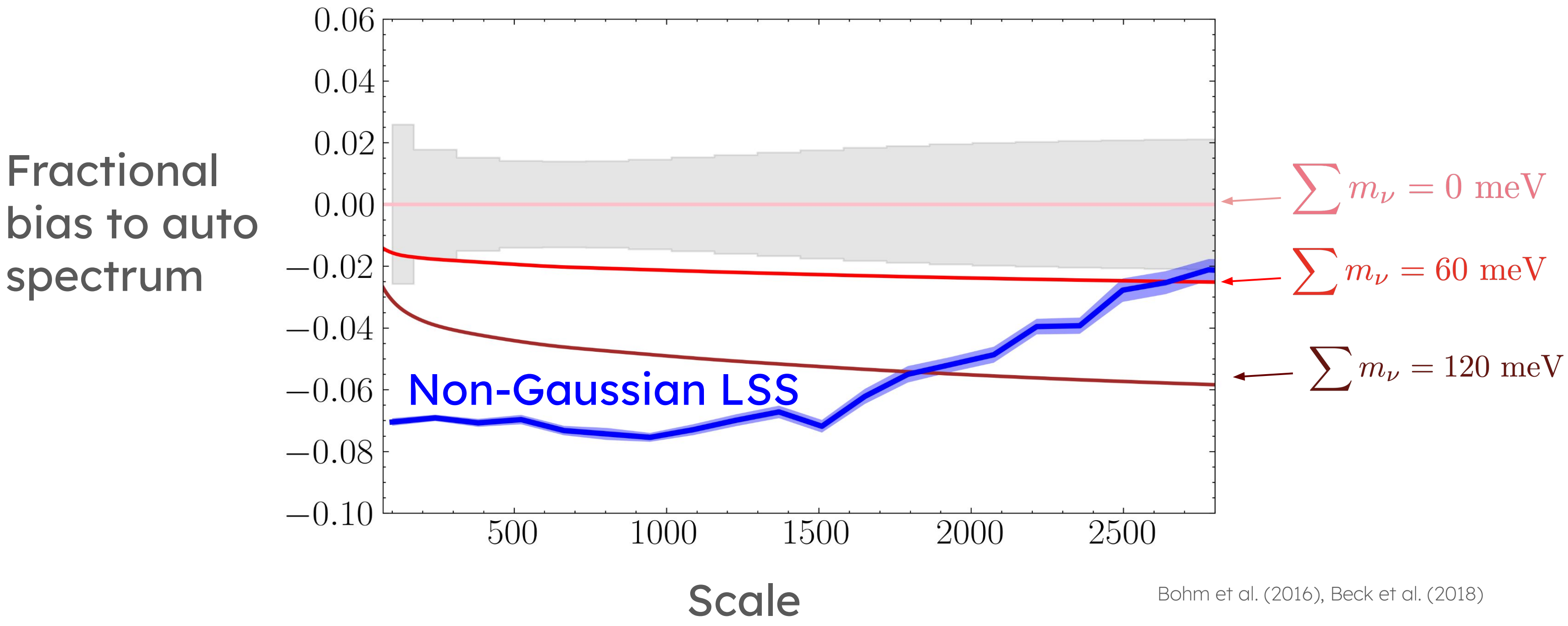

Bohm et al. (2016), Beck et al. (2018)

Impact of non-Gaussian deflections

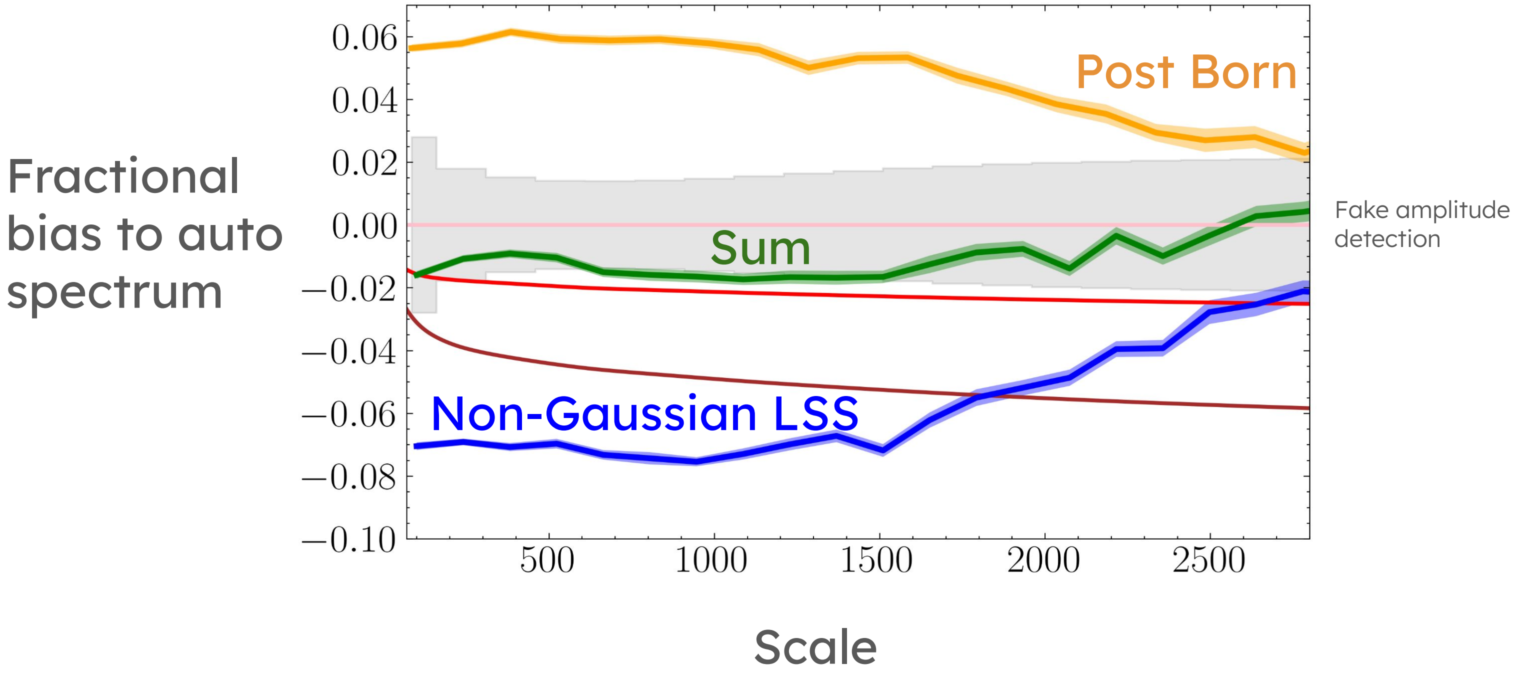

The QE CMB lensing estimator

$$\hat{\kappa}_{\mathrm{QE}} \sim \bar{X}^{\mathrm{dat}}\,\bar{X}^{\mathrm{dat,WF}} \times \mathrm{Norm}$$

by construction misses info in $\phi^2,\ \ldots.$

but also $XXX,\ XXXX,\ \ldots$

Impact of non-Gaussian deflections

Fractional bias to auto spectrum

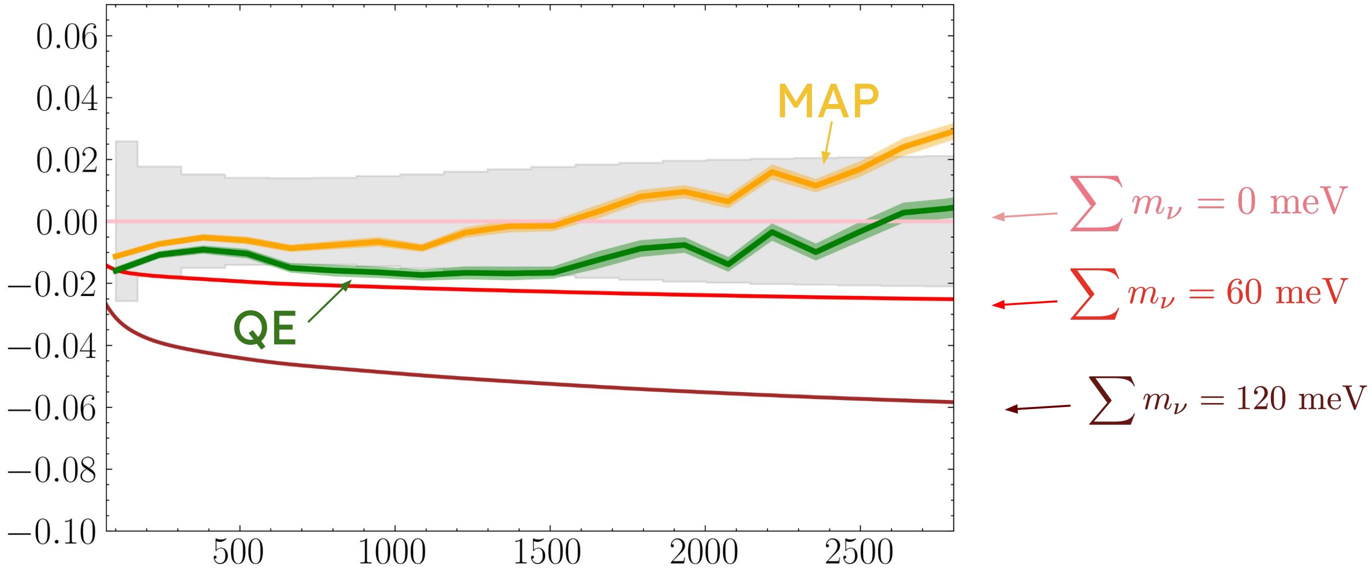

Scale

Impact of non-Gaussian deflections

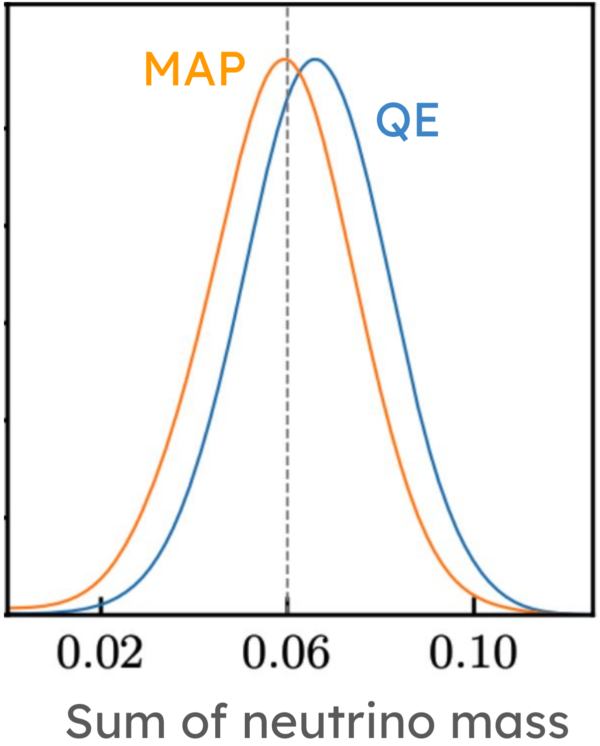

Improved QE likelihood treatment compared to past work

Impact of non-Gaussian deflections

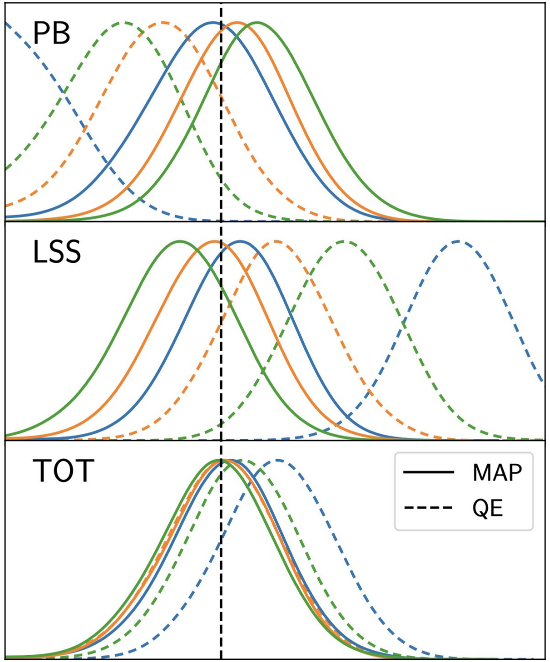

Sum of neutrino mass

Important for CMB lensing cross-correlations

Nice cancellation for CMB lensing auto-correlation

Conclusions

- **Key goal of CMB-S4 is sum of neutrino masses**
- non-Gaussian effects skew inference for QE
- Optimal methods improve upon standard ones
- Explored alternative estimators
- Cross-correlations with large scale structure

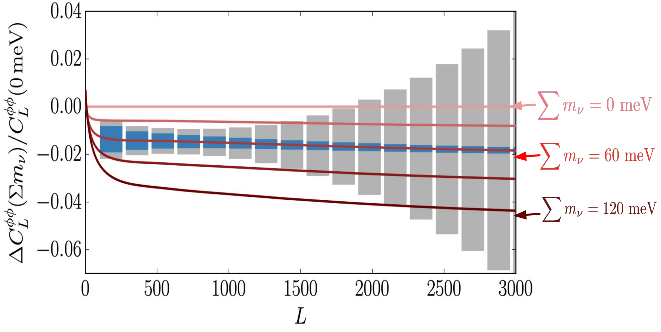

o.darwish@proton.me

Extras

Joint Potential-Curl reconstruction

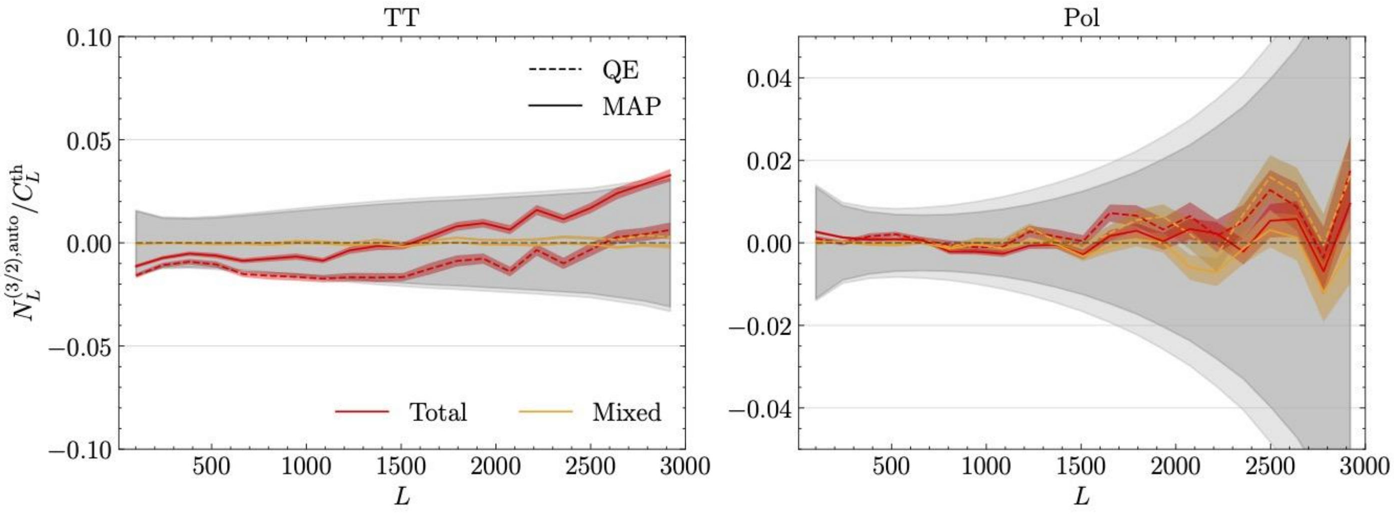

Impact of non-Gaussian deflections

Fractional bias to auto spectrum

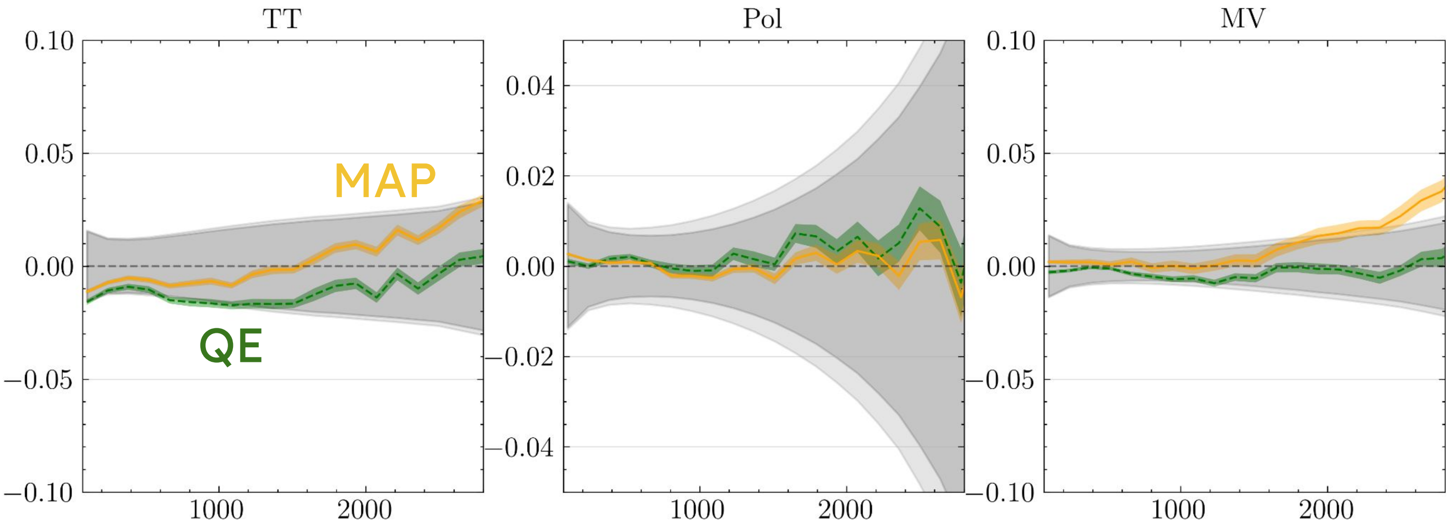

Scale

Comparing likelihoods

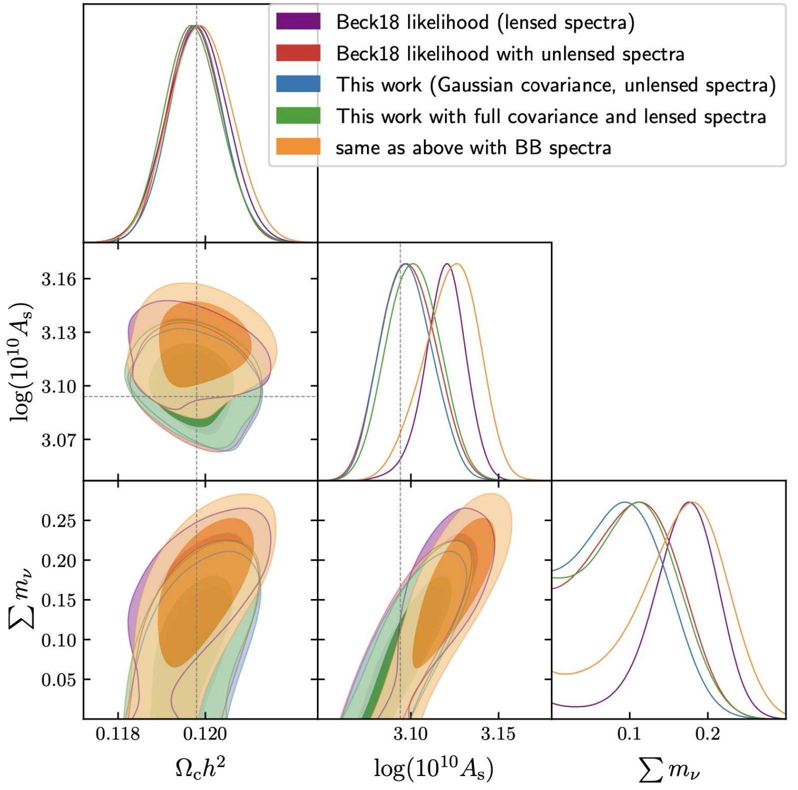

Alternative estimators, LSS Case

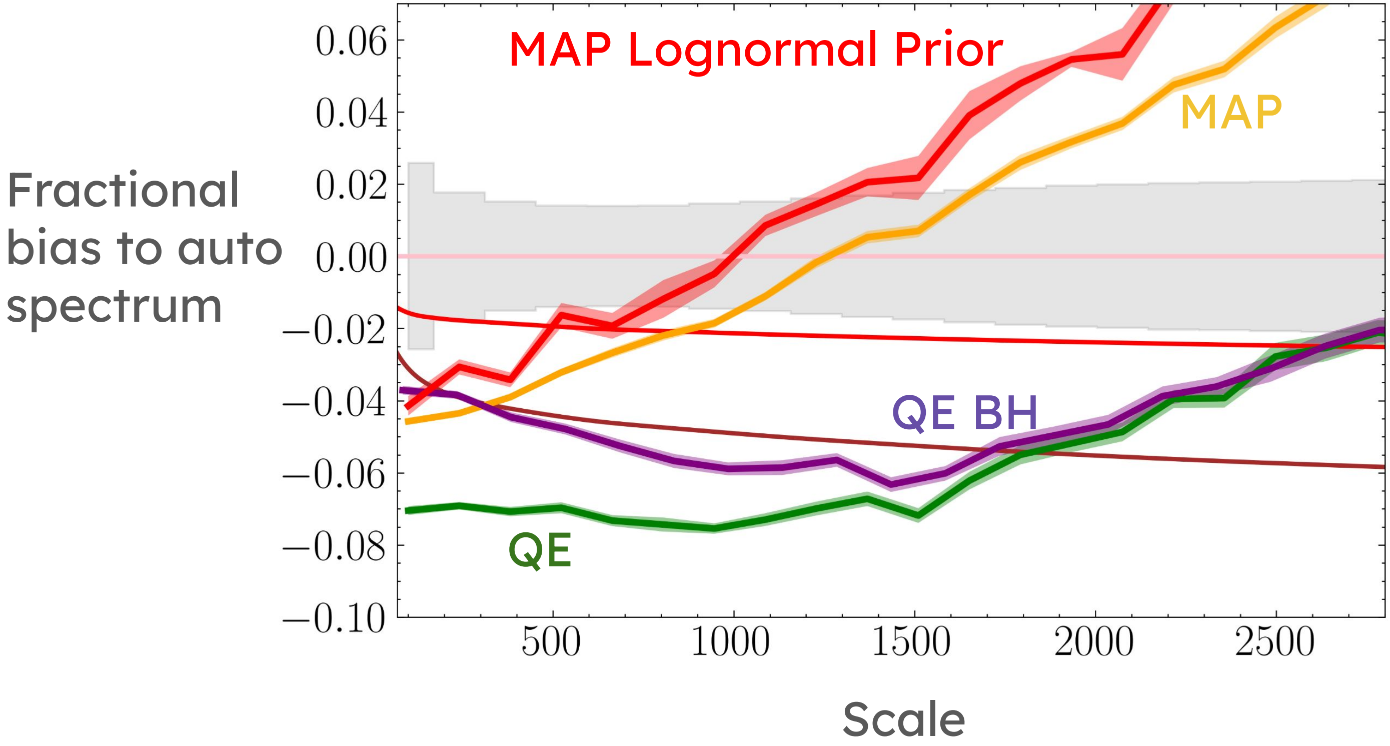

Cross-correlations with QE

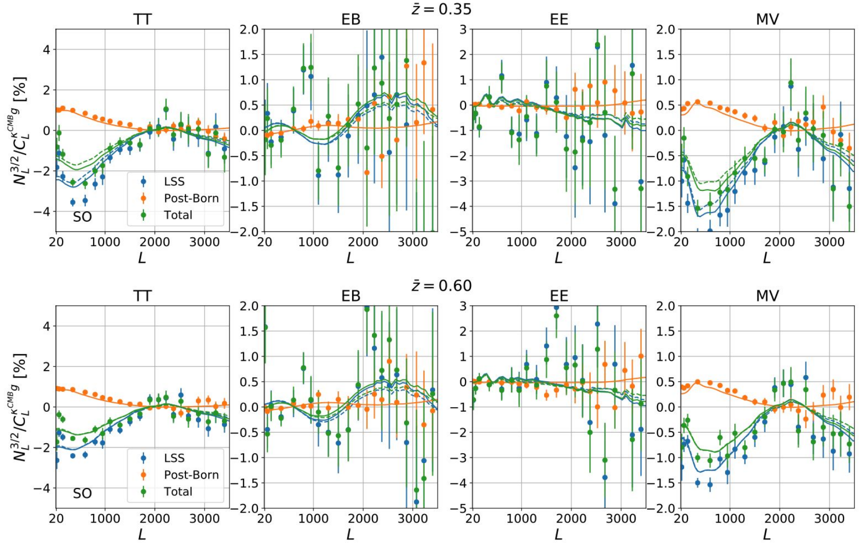

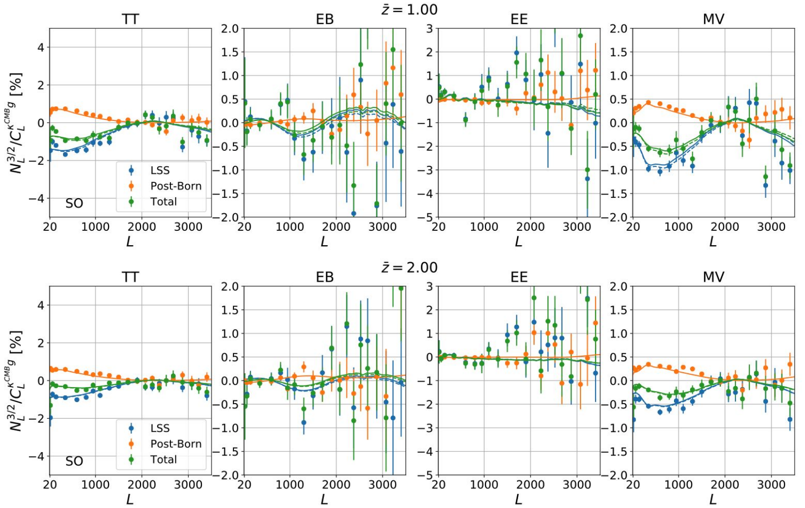

Figure 12: Fractional $N_L^{(3/2)}$ bias for the cross-correlation power spectrum between the reconstructed CMB lensing potential of SO and galaxy density at different redshift bins. The redshift increases moving from top to bottom. Theoretical predictions using GM fitting formulae for the matter bispectrum are shown as solid lines while those based on SC fitting formulae are shown as dashed lines. Different contributions to the $N_L^{(3/2)}$ signal are shown in different colours. The error bars accounts for the sample variance of CMB alone.

Cross-correlations with QE

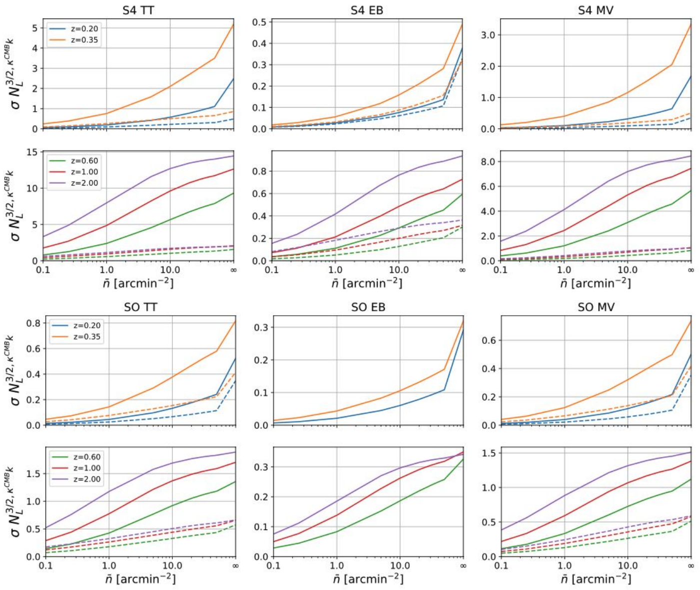

Figure 15: Detection significance of $N_L^{(3/2)}$ measured in simulations for cross-correlation between the reconstructed CMB lensing and galaxy lensing as a function of the shot noise in an LSS survey (solid). Results for S4 (SO) are shown in the upper (lower) panels. LSST/Euclid-like surveys have $\bar{n} \approx 3$, depending on the bin thickness. Different reconstruction channels are shown from left to right, while different redshift bins are shown in different colours. The dashed lines show the detection significance σ of the residual $N_L^{(3/2)}$ bias after subtraction of the analytical prediction of this work (using GM fitting formulae gives consistent results).

QE CMB lensing estimator

$$\ln \mathcal{L} \supset -\frac{1}{2} X^{\mathrm{dat}} \cdot \mathrm{Cov}_{\vec{\kappa}}^{-1} X^{\mathrm{dat}} - \frac{1}{2} \det \mathrm{Cov}_{\vec{\kappa}}$$

$$\Big\Downarrow \text{ Maximize}$$

$$\hat{\kappa}_{\mathrm{QE}} \sim \vec{\nabla} \cdot \left[\bar{T}_{\mathrm{lensed}} \vec{\nabla} \bar{T}^{\mathrm{WF}}_{\mathrm{lensed}} \right] \times \mathrm{Norm}$$

First step of a Newton iteration starting from no lensing